AIAA AVIATION Forum
June 25-29, 2018, Atlanta, Georgia
2018 Applied Aerodynamics Conference

10.2514/6.2018-3960

Study on a Camber Adaptive Winglet

João Paulo Eguea* and Fernando Martini Catalano† and Alvaro Martins Abdalla‡
University of São Paulo, São Carlos,São Paulo,1566-590

Leandro de Santana§ and Cornelis H. Venner¶
University of Twente, Drienelolaan 5, 7522 NB, Netherlands

André Luiz Fontes Silva‖
EMBRAER, Av. Brg. Faria Lima 2170, São José dos Campos-SP,Brazil

Morphing structures are devices intended to be implemented in specific parts of the aircraft such to improve some aspects of the flight such as performance and maneuverability. More specifically for the wings, the in flight capability of adaptation of airfoil profile and control surfaces bring possibility to the aircraft operate at optimum performance condition during all flight phases. Morphing structures can only lead to optimal flight maneuverability and performance conditions if the morphed geometry leads to an improved flight condition. Aiming at the reduction of the lift induced drag in all flight phases, this research focus on the application of the genetic optimization algorithm for the definition of the camber section of an winglet. This research proposes the optimization at four different flight phases namely: climb, heavy cruise, mid cruise and light cruise. BLWF – a full potential equation solver coupled with 3D boundary layer modelling – is adopted in the aerodynamic performance, e.g. lift and drag ratio, calculation. A conventional genetic algorithm is adopted in the optimization of the camber of the airfoil composing the winglet. This paper describes the optimization procedure and compares geometries showing that the in flight change of the winglet geometry can sensibly contribute to the improvement of the aircraft performance reducing the fuel consumption.

I. Nomenclature

a_{le}	=	leading edge parameter
a_{te}	=	trailing edge parameter
C_D	=	drag coefficient
C_{D_total}	=	total drag coefficient
$C_{D_induced}$	=	induced drag coefficient
C_L	=	lift coefficient
D	=	drag
h	=	flight altitude
L	=	lift
Mach	=	Mach number
M_∞	=	Mach number at infinity
RC	=	rate of climb
T	=	thrust
u_n	=	normal velocity component
V	=	airplane true speed
W	=	aircraft weight
W_{final}	=	aircraft final weight on cruise

*BSc, Department of Aeronautics Engineering, Av. Trabalhador São Carlense 400, São Carlos-SP, Brazil.
†Professor, Department of Aeronautics Engineering EESC-USP, Av. Trabalhador São Carlense 400, São Carlos-SP, Brazil, AIAA Member.
‡PhD, Department of Aeronautics Engineering EESC-USP, Av. Trabalhador São Carlense 400, São Carlos-SP, Brazil.
§Assistant Professor, Faculty of Engineering Technology. Department of Engineering Fluid Dynamics, AIAA Member.
¶Professor, Faculty of Engineering Technology. Department of Engineering Fluid Dynamics.
‖MSc, EMBRAER, Av. Brg. Faria Lima 2170, São José dos Campos-SP,Brazil

$W_{initial}$ = aircraft initial weight on cruise
α_f = final angle of attack
α_i = initial angle of attack
$\Delta\alpha$ = angle of attack variation
$\eta_{overall}$ = propulsion efficiency
ρ = air density

II. Introduction

Winglets are wing tip devices adopted to reduce the lift induced drag by changing the wing tip vortex structure. The lift induced drag component can correspond for 40% up to 80% of total drag in cruise and climb conditions, respectively [1]. However, winglets also increase the viscous drag component and structural weight leading to a negative impact on the aircraft performance. Computational and wind tunnel investigations show that winglets considerably increase aircraft performance even when the viscous drag and structural changes are considered [2–7].

Morphing structures can increase the overall aerodynamic efficiency and control capabilities [8–12] and morphing winglets showed good results [13–16] improving the wing lift to drag ratio.

A camber morphing winglet aims at reducing the winglet aerodynamic loading accordingly to the flight condition. The camber alterations would reduce the pressure drag on the winglet for conditions of lower lift, when the induced drag component is smaller, reducing the drag component penalty in this flight phase. Optimizing the winglet geometry for different flight condtions would bring reduction of the airplane total drag, improving the aircraft performance. Martins and Catalano [17] developed a morphing mechanism capable of changing the angle of the leading and trailing edge of the airfoil fixing the central part, see Fig. 1. This mechanism aims at improving the winglet stiffness and system integrity keeping the main structural box intact. This design makes the camber morphing winglet feasible for real applications in the aeronautical industry. The morphing system used in this study is similar to the one used by Cosin et al. [18]. Figure 2 shows an image from the constructed morphing system.

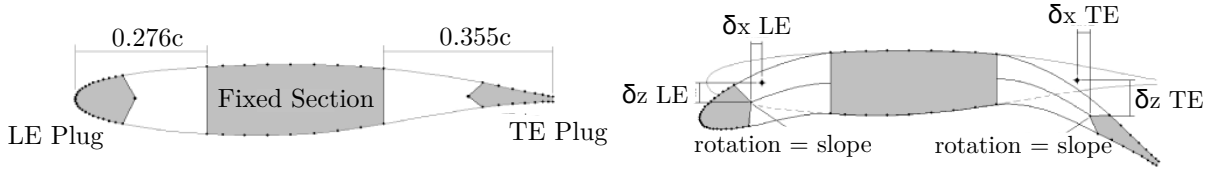

(a) Morphing wing in the stowed configuration (b) Morphed section representation

Fig. 1 Winglet morphing device scheme [17].

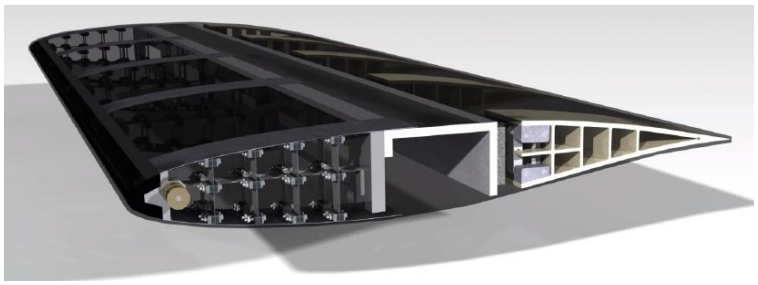

Fig. 2 Designed morphing system drawing [18]

This paper adopts a genetic algorithm in the optimization of four different winglets to be applied in different flight phases. A Genetic Algorithm (GA) is a meta heuristic method able to find a near optimum solution for a problem independently of the nature of the problem or the shape of the objective function. This method is suitable for complex and multidisciplinary problems, being widely used for wing geometry optimization.

Cosin et al. [18] adopted a genetic algorithm to optimize the camber geometry of a morphing wing aiming at minimizing the wing total drag. Smith et al. [13] adopted a multi-objective genetic optimization aiming at improving

adaptive cant angle of the wing tip for a commercial transport jet. Smith's analysis improved range and reduced the aircraft's take-off and landing distances. Cayiroglua and Kilic [19] combined a genetic algorithm with CFD and finite elements structural analises to optimize a wing geometry composed by NACA 4-digit airfoils sections. Holst and Pulliam [20] implemented a genetic algorithm coupled with a full potential aerodynamic model to optimize a transonic wing section for single and multi-objective shape optimization.

The genetic algorithm is a powerful optimization tool applicable to problems of different nature. This algorithm relies on the capacity of the external solver performing accurate prediction in the entire searching space defined by the individuals to be selected in the algorithm. In the specific case analysised in this research, the capability of convergence of the genetic algorithm towards an optimum solution of physical meaning largely relies on the aerodynamic model fidelity. Therefore, the choice of the aerodynamic solver is decisive to the representativity of the optimization process. Based on this consideration this research adopts the BLWF solver. BLWF is a a full potential aerodynamic model, is used for evaluation of airplanes including the capability of considering different winglet configurations. This code, developed at the Central Aerohydrodynamic Institute (TsAGI), provides fast and reliable results in analysis at transonic flow regime and complex wing-body-winglet configurations. This research implements an experimental campagin aiming to validate the aerodynamic results provided by BLWF. In this analisis, four wing+winglet models are 3D printed representing the optimized geometries for climb, heavy, mid and light cruise conditions. The lift and drag compoments are tested for all models and the experimental results are compared to BLWF simulations.

III. Methodology

A. Aircraft geometry

A generic mid-size business jet shown in Fig. 3 is chosen as the base geometry in this development. For this optimization process a wing-fuselage configuration is used.

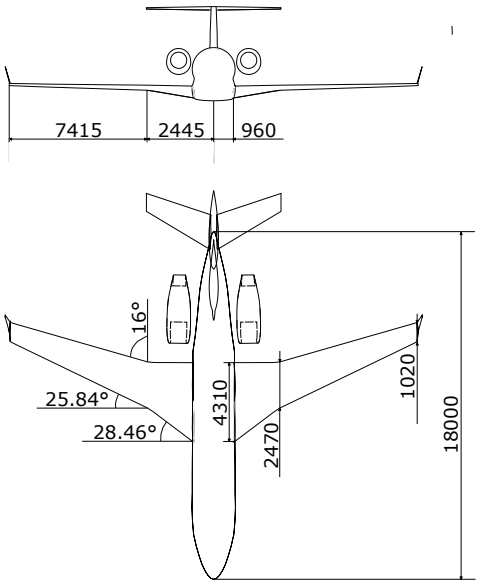

Fig. 3 Airplane geometry. Linear dimensions are represented in millimeters and the angles in degrees.

Five control sections along the winglet span are select to place the morphing airfoil. The span position of the sections are based on the winglet coordinate system defined in Fig. 4 are shown in Tab. 1. The airfoil sections camber changes are based on the morphing mechanism developed by Martins and Catalano [17]. In this proposed construction, the airfoil sections are able to change the leading and trailing edges angles. The angles are constrained by the maximum angles that the system can bend and still create a smooth surface, Fig. 2. The leading and trailing edge parameters are contained in the interval $-0.1 \leqslant a_{le} \leqslant 0.05$ and $-2.45 \leqslant a_{te} \leqslant 1.3$, respectively. BLWF is able to simulate winglet geometries defined at any point of a_{te} and a_{le} interval.

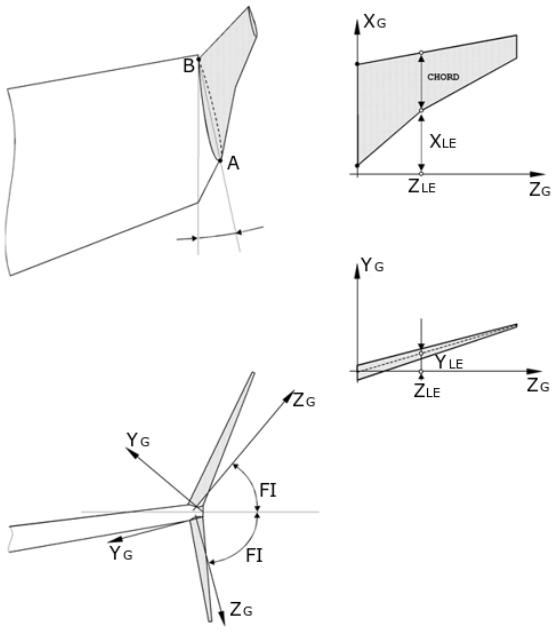

Fig. 4 Coordinates system adopted in the Winglet analises.

Table 1 Coordinates of the winglet sections.

Section	X_{LE} [m]	Y_{LE} [m]	Z_{LE} [m]	Chord [m]
1	0.00000	0.000	0.000	0.5500
2	0.12058	0.000	0.178	0.4804
3	0.27705	0.000	0.409	0.3901
4	0.48027	0.000	0.709	0.2728
5	0.74513	0.000	1.100	0.1200

B. Aerodynamic model

BLWF [21] solves the full potential equation coupled with 3D boundary layer calculation [22], allowing fast solutions of complex transonic flows. The conservative full potential equations are presented by Jameson and Caughey [23]. BLWF adopts continuity of the velocity potential, implying continuity of the tangential velocity component and continuity of ρu_n are set as conditions of the shock jump. No conservation of the normal moment component through the shock wave under the isentropic assumption is taken. This imbalance produces a body force that is an approximation to the wave drag. Jameson and Caughey [23] presents the finite volume methodology used to solve the full potential equations. The 3D boundary layer coupled method used on the software is described McLean and Randall [24]. BLWF has a mesh generation method described by Yu [25].

Zhang and Hepperle [26] studied the BLWF application in aerodynamic simulations of wing-body configurations subjected to transonic flow conditions. BLWF estimates aerodynamic coefficients with acceptable uncertainty for preliminary design.

C. Optimization process

The genetic algorithm is an evolutionary algorithm, searching for an optimum solution from an initial random population. Every individual is evaluated by calculating a fitness factor defined by an objective function that determines the fit of individuals to the aimed scenario. In the present study, the winglets are evaluated in four different conditions: climb, heavy, mid and light cruise. The flight speed, altitude and lift for the studied conditions are shown in Tab. 2.

Table 2 Typical flight conditions considered in the optimization.

Condition	Altitude [ft]	Mach [-]	C_L []
Climb	30000	0.60	0.5150
Heavy cruise	45000	0.75	0.4885
Mid cruise	45000	0.75	0.4525
Light cruise	45000	0.75	0.4165

The objective function defined for the climb flight phase is set such to maximize the airplane rate of climb. Based on the climb performance equations defined by Roskan [27], the rate of climb depends on the inverse of $\frac{C_L}{C_D}$ (Eq. 1). The climb condition optimization is maximizes the objective function shown in Eq. 2. A geometrical constrain was set such to impose that the angle of the leading or trailing edges are equal or larger than the angle of the previous section, avoiding convergence to optimal geometries that could not be reproduced in a real application.

$$RC = \frac{(T-D)V}{W} = (\frac{T}{W} - \frac{D}{W})V = (\frac{T}{W} - \frac{D}{L})V \tag{1}$$

$$Fitness_{Climb} = 10\frac{C_L}{C_D} \tag{2}$$

The cruise condition optimization aims to maximize the range. The Breguet's range equation (Eq. 3) shows that the range is proportional to the lift to drag ratio. The cruise condition optimization targets to maximize the objective function shown in Eq. 4.

$$Range = \frac{h}{g}\frac{L}{D}\eta_{overall} \ln \frac{W_{initial}}{W_{final}} \tag{3}$$

$$Fitness_{Cruise} = 10\frac{C_L}{C_D} \tag{4}$$

The fitness factor determine the probability of an individual to reproduce. The better fitted individuals have higher probability of being selected for reproduction. A percentage of the best individuals are selected as part of the next generation (elitism). The individuals are selected for reproduction randomly using a roulette wheel selection. On reproduction the selected individuals exchange parts of their gens (crossover) and random changes on the gen structure (mutation). The new generation is evaluated again using the objective function. The method is considered converged when the worse and best individuals on the population have the same fitness. Further information about genetic algorithms can be found in Goldberg [28].

The first author of this paper developed the algorithm, which was validated by optimization problems with known solutions, such as known polynomial objective function and wing weight optimization varying wing tapper and aspect ratio. A study of the minimum initial population is performed to ensure that the final result corresponds to the optimum solution. Populations of sizes $100n$ are tested for $10n^{th}$ generations in the winglet optimization for mid cruise condition and compared such to determine the minimum population size that ensures convergence. Elitism and mutation rate are defined based on stability and convergence analyses. Results presented in Fig. 5 and Tab. 3 show that for a population of 300 individuals the converged solution is the same for simulations with larger initial populations with differences of up to 0.0012% which implies negligible difference in the airplane's $\frac{C_L}{C_D}$ ratio. The computational time is directly proportional to the population size, once the aerodynamic simulation of each individual is the most time consuming phase of the process. Based on this analysis a population of 300 individuals is adopted such to ensure convergence to a global optimum with minimal computing time.

Table 3 Fitness relation with population size showing the minimum size for optimum convergence

Population size	100	300	500	600
Fitness	130.4245	133.1458	133.1473	133.1431

The morphing mechanism is capable to change the leading and trailing edge angles of the five selected winglet sections [17]. The population individual's gens are composed by 40 bits. Each group of 4 bits form a binary number

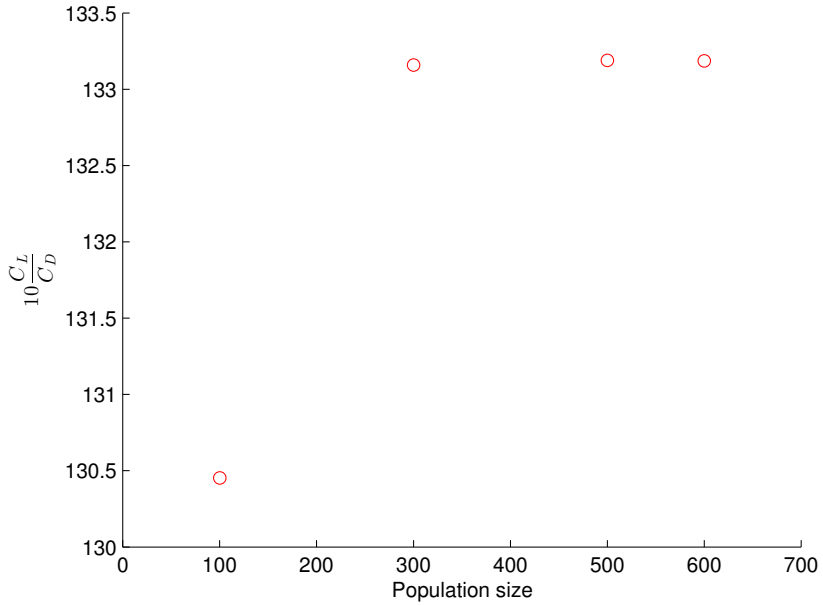

Fig. 5 Analysis of the population size showing the minimum size for optimum convergence.

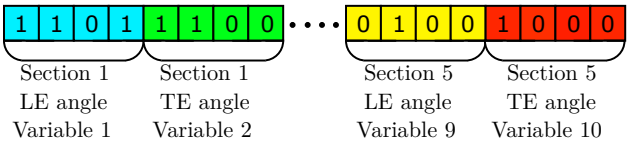

Fig. 6 Binary representation of population individual genetic code structure and optimization variables

that represent the angle of the trailing or leading edge of one winglet section. Therefore, the genetic algorithm works optimizing a group of 10 variables, see Fig. 6.

Thierens and Goldberg [29] showed a study on the minimal population size (n) and generations (g_{conv}) necessary to ensure convergence towards a global optimum. Equations 5 and 6 gives the relation between n and g_{conv} with the gen length (l), represented in Fig. 6. The gen length for the winglet optimization presented in this paper is $l = 40$, therefore $n = 80$ and $g_{conv} = 18$ is a reasonable population sizes and number of generations for achieving global optimum convergence. Table 4 shows the parameter used for the genetic optimization. The chosen parameters of this analysis are higher than those suggested by Thierens and Goldberg [29] such to ensure proper convergence.

$$n = 2l \tag{5}$$

$$g_{conv} = \frac{\pi}{2}\sqrt{\pi l} \tag{6}$$

Table 4 Parameters adopted in the genetic optimization.

Population size	Gen length	Number of variables	Mutation rate [%]	Elitism [%]
300	4	5	0.25	5.0

D. Wind tunnel experiment

Wind tunnel measurements are performed aiming at assessing the influence capacity of BLWF of reproducing physically meaningful results and to investigate the influence of different winglets on the lift induced drag. Aerodynamic

measurements on the lift, drag and pitching moment were performed in a open circuit closed test section wind tunnel at University of São Paulo. The test section dimensions are 1.05 x 0.8 m^2 and 2.1 m long.

A circular end plate is adopted to minimize wall effects on the wing root of the model. An extra measurement is performed adopting only an end plate such to subtract its effects from the raw data. The angle range is chosen such to find the zero lift angle and stall characteristics of all configurations tested. The velocity was set to the wind tunnel maximum speed (Tab. 5).

Table 5 Wind tunnel experiment conditions.

α_i	α_f	$\Delta\alpha$	V [m/s]
−6°	20°	1°	25

The wing and winglets are prototyped using fuse deposition material Stratasys Fortus 360 MC printer at University of São Paulo. Primer finishing is applied to the models followed by a black paint and a water sanding process to improve the surface finishing. A trip strip is added to all surfaces at 10% of the local chord to force boundary layer transition.

IV. Results

A. Winglet optimization

The winglet optimization is performed considering the aforementioned flight conditions. The fitness of the best and worst individuals in each generation and mean fitness of the population along the generations is shown in Fig. 7. After 30 generations the best individual fitness is almost constant. Therefore, the optimization process stopped and the best individual, after 30 generations, and taken as the optimum solution.

Table 6 shows the drag coefficient component of the baseline and optimized camber morphing geometry. A reduction in the drag coefficient of up to -0.58% is observed. The airfoil sections evolution of the best, median and worst individuals on the population for all configurations are shown in Fig. 8 to 19. The camber adaptive winglet is able to improve the airplane performance when compared to the baseline fixed geometry winglet.

Table 6 Drag components for different conditions.

	Baseline		Optimum configuration		
Condition	$C_{D_{total}}$ [-]	$C_{D_{induced}}$ [-]	$C_{D_{total}}$ [-]	$C_{D_{induced}}$ [-]	$\%\Delta C_D$
Climb	0.03774	0.00750	0.03752	0.00742	-0.58
Heavy cruise	0.03626	0.00665	0.03625	0.00661	-0.03
Mid cruise	0.03432	0.00586	0.03427	0.00582	-0.15
Light cruise	0.03218	0.00499	0.03213	0.00496	-0.16

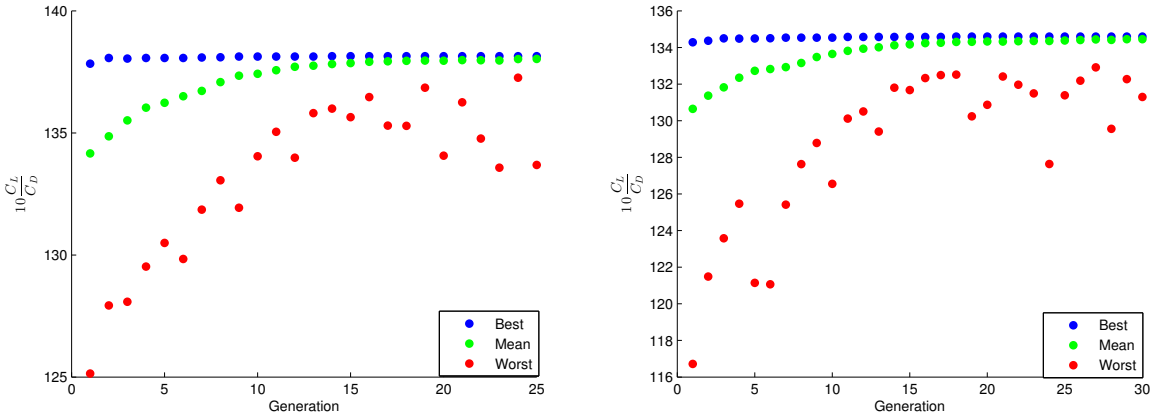

(a) Climb condition

(b) Heavy cruise condition

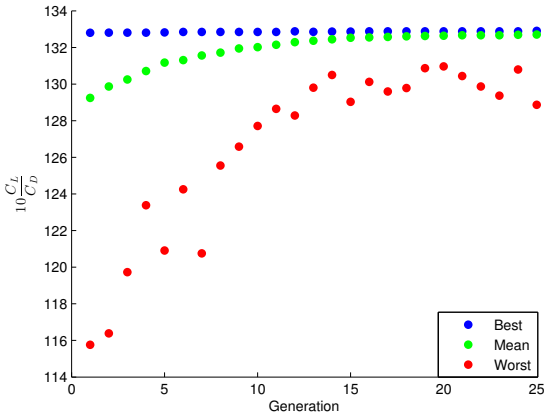

(c) Mid cruise condition

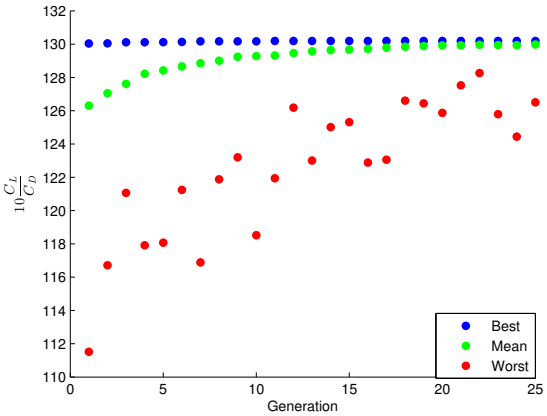

(d) Light cruise condition

Fig. 7 Individuals fitness per generation for different flight conditions optimizations

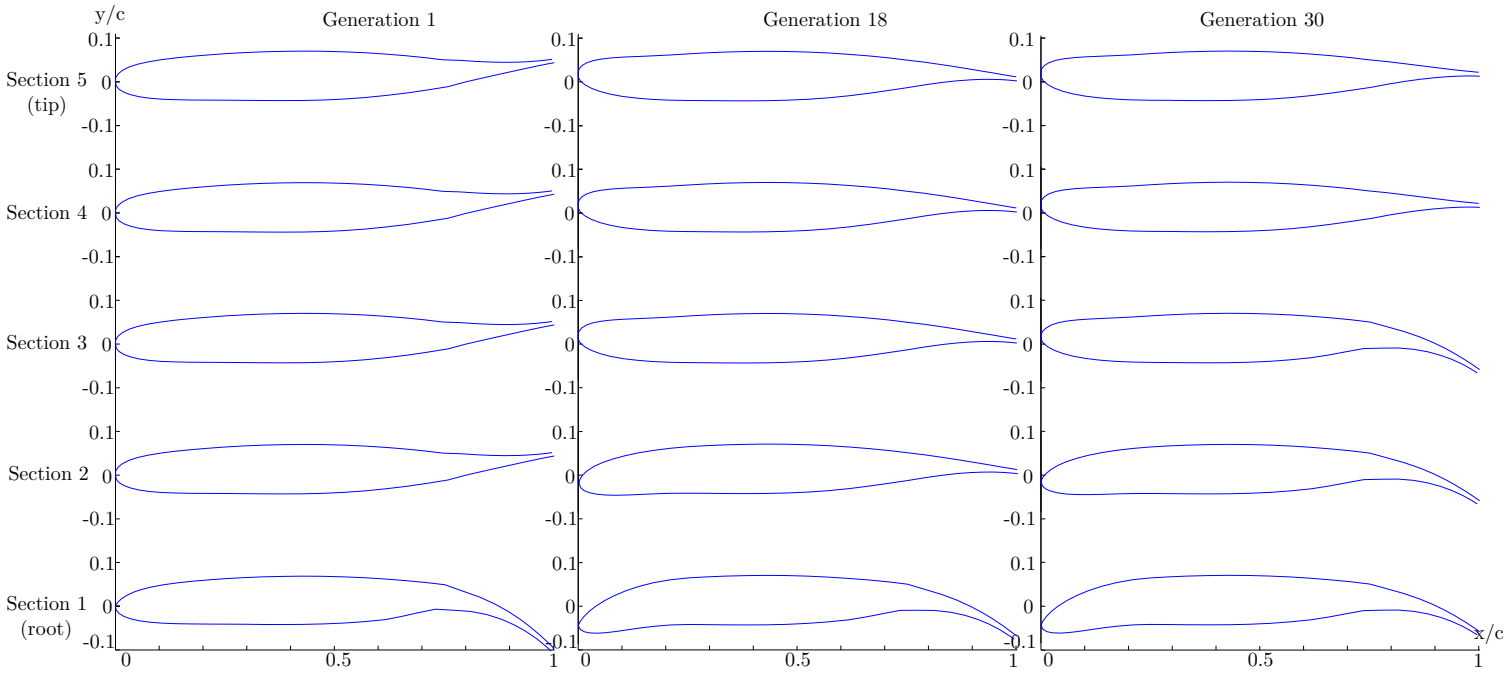

Fig. 8 Climb worst individual evolution.

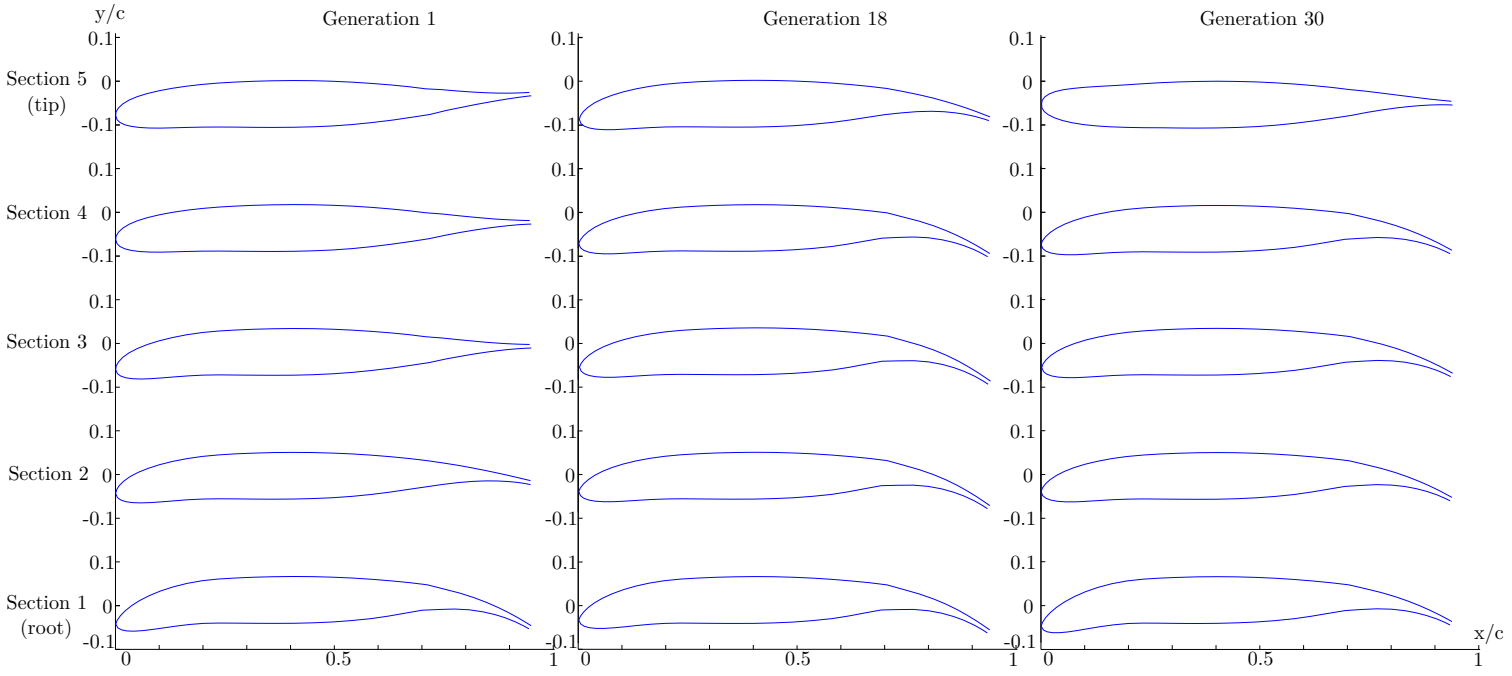

Fig. 9 Climb median individual evolution.

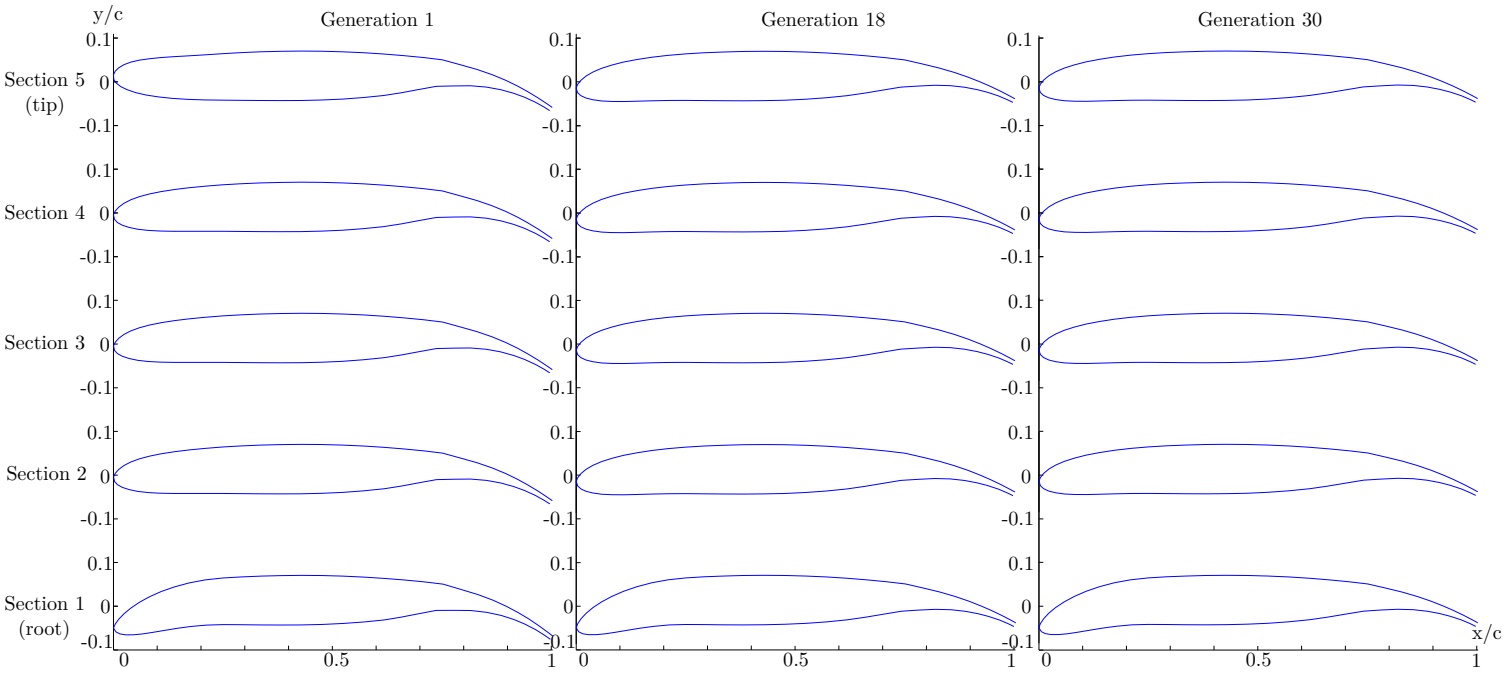

Fig. 10 Climb best individual evolution.

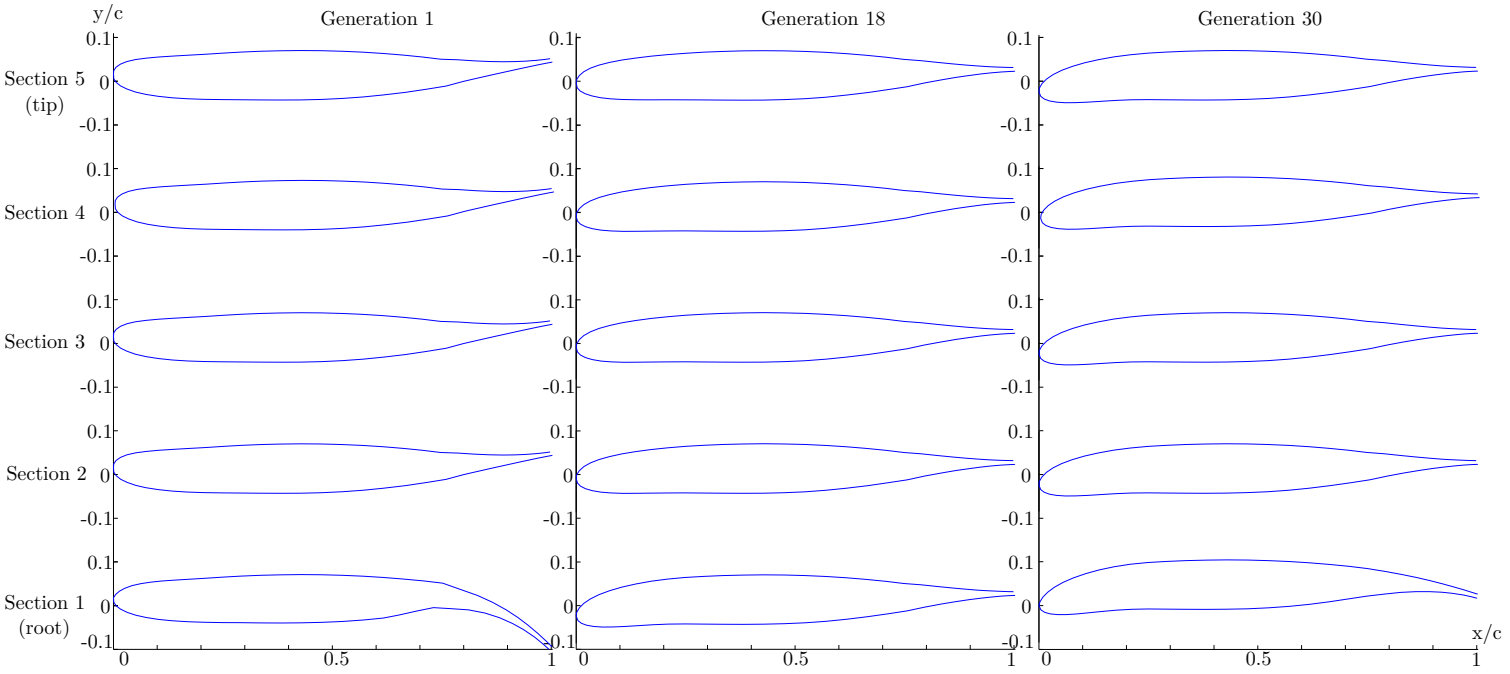

Fig. 11 Heavy cruise worst individual evolution.

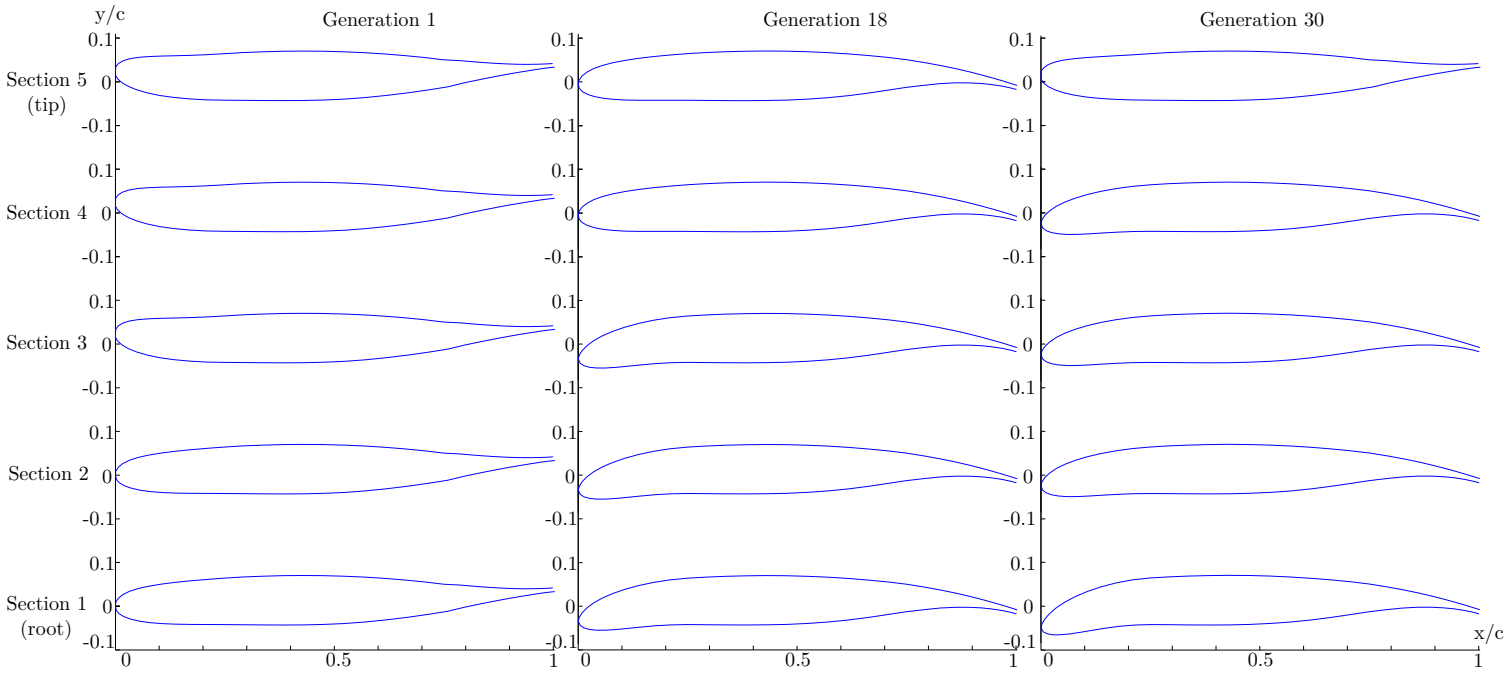

Fig. 12 Heavy cruise median individual evolution.

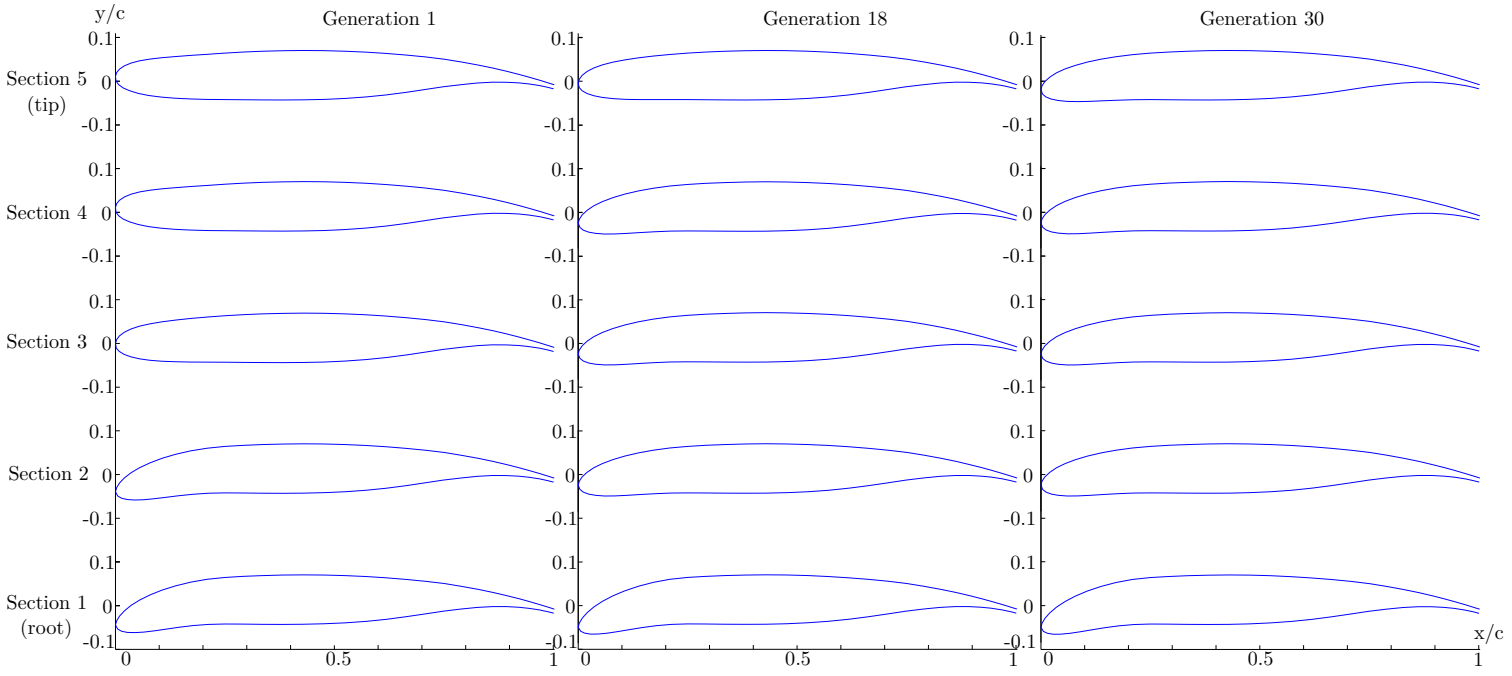

Fig. 13 Heavy cruise best individual evolution.

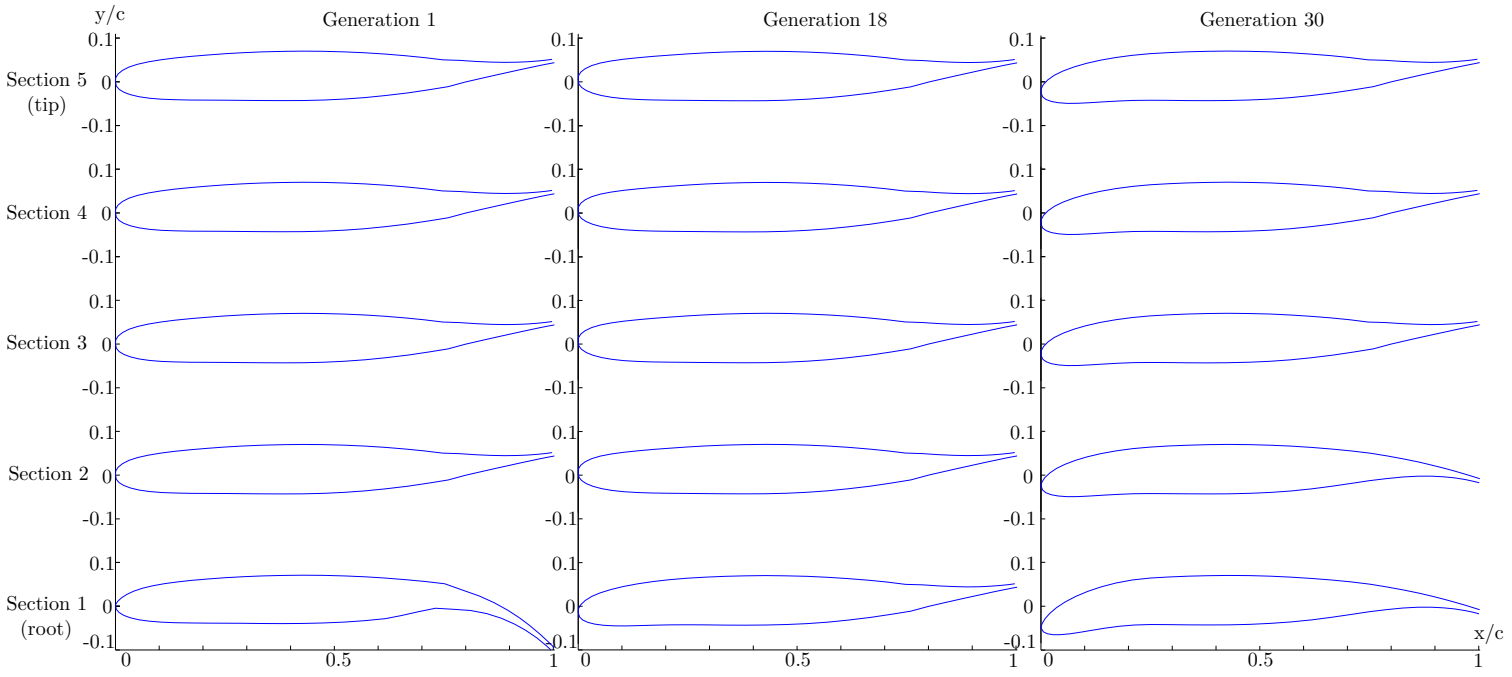

Fig. 14 Medium cruise worst individual evolution.

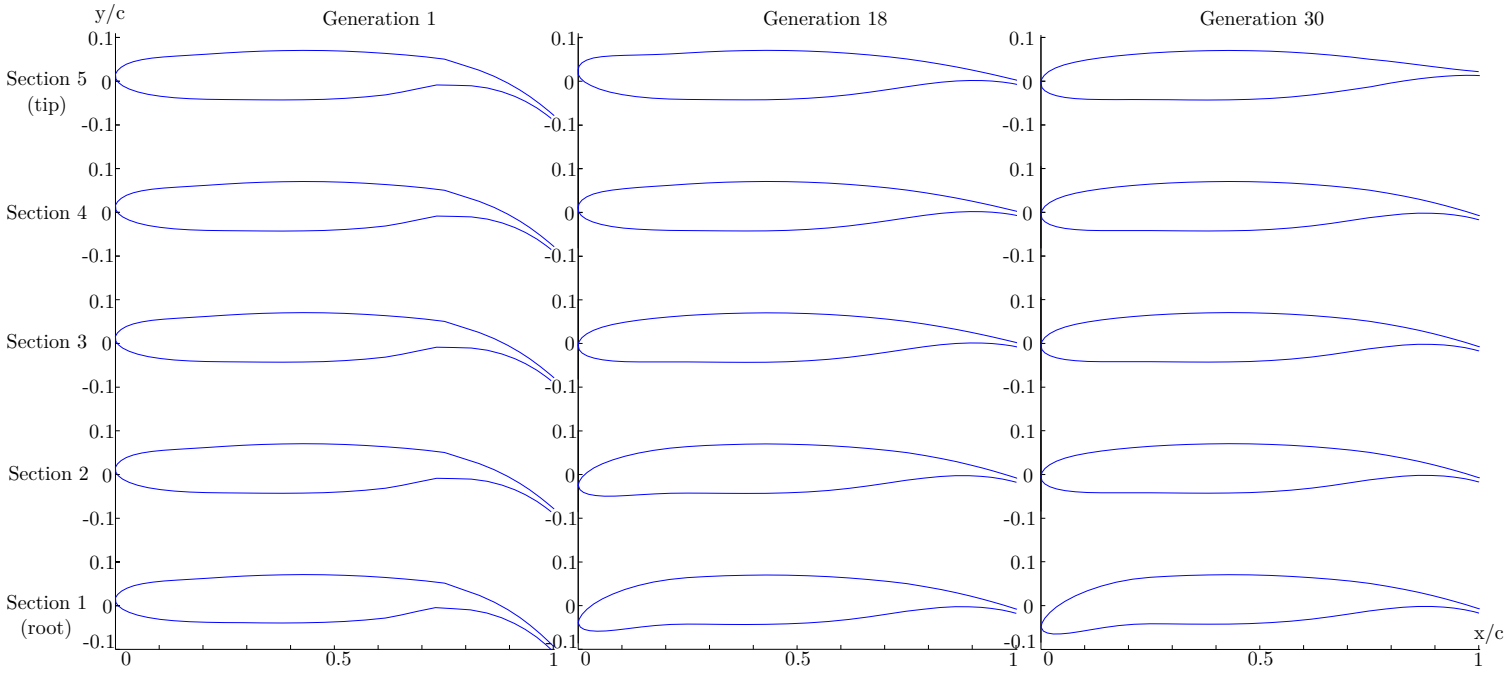

Fig. 15 Medium cruise median individual evolution.

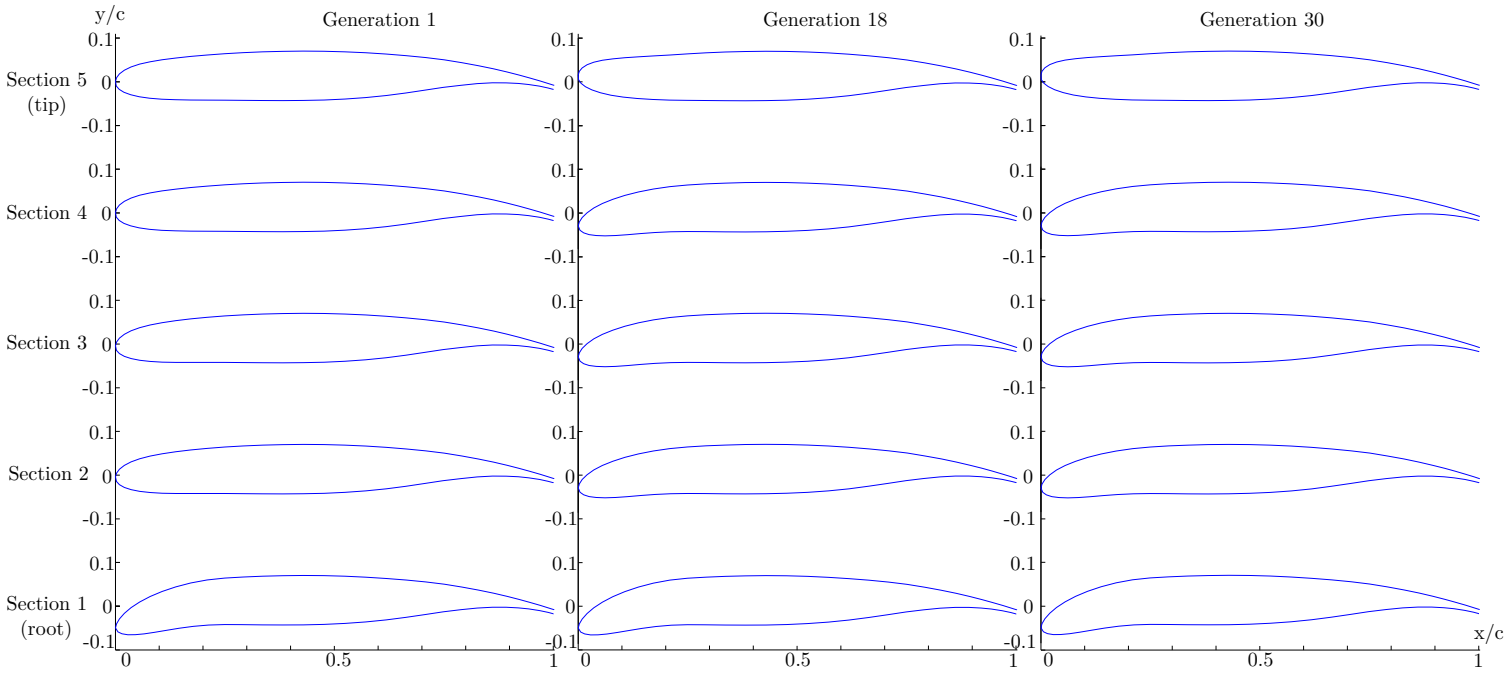

Fig. 16 Medium cruise best individual evolution.

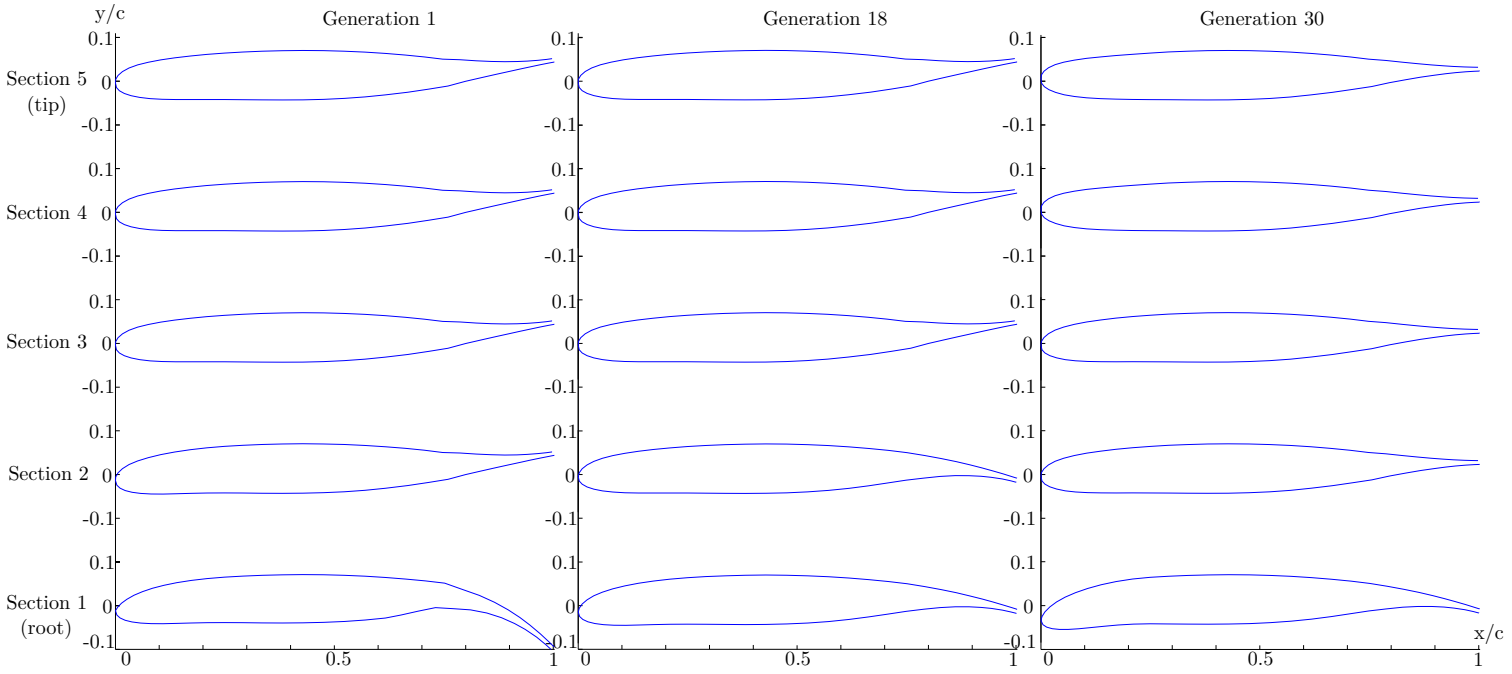

Fig. 17 Light cruise worst individual evolution.

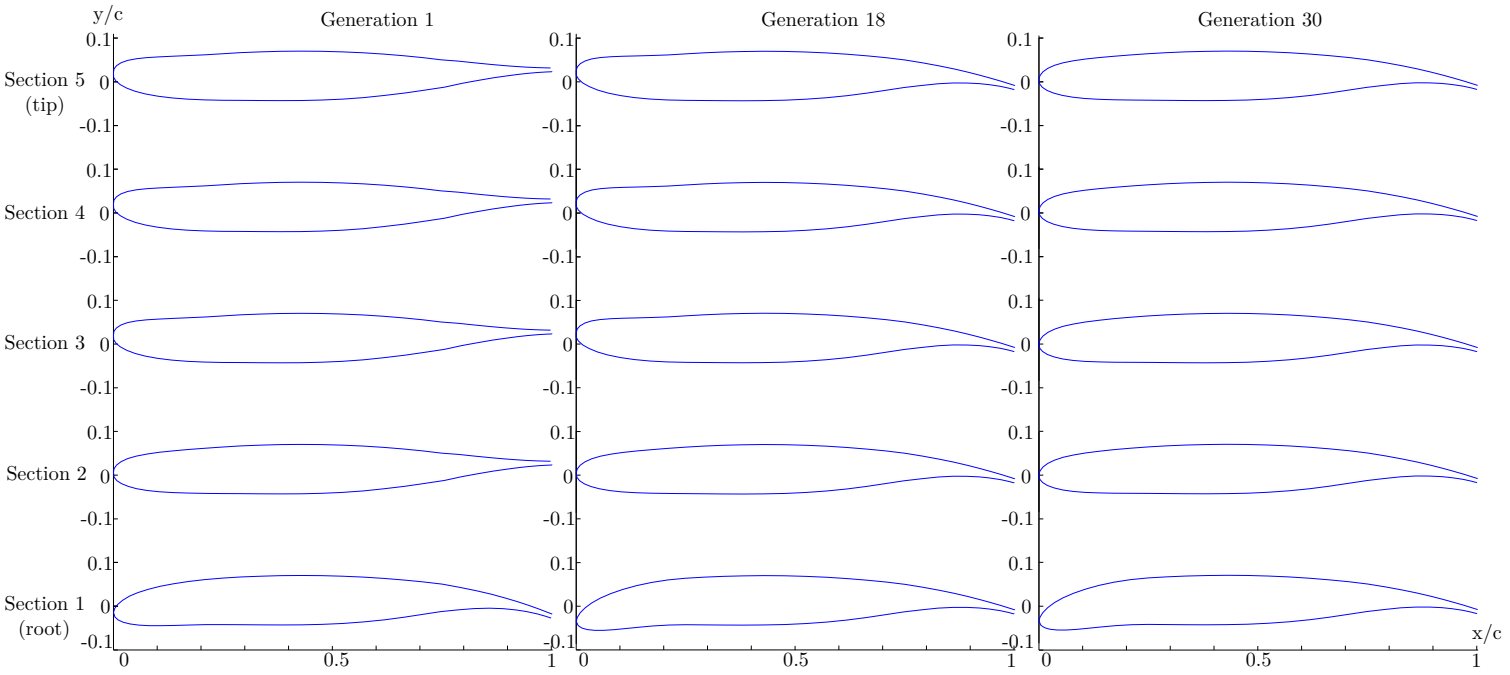

Fig. 18 Light cruise median individual evolution.

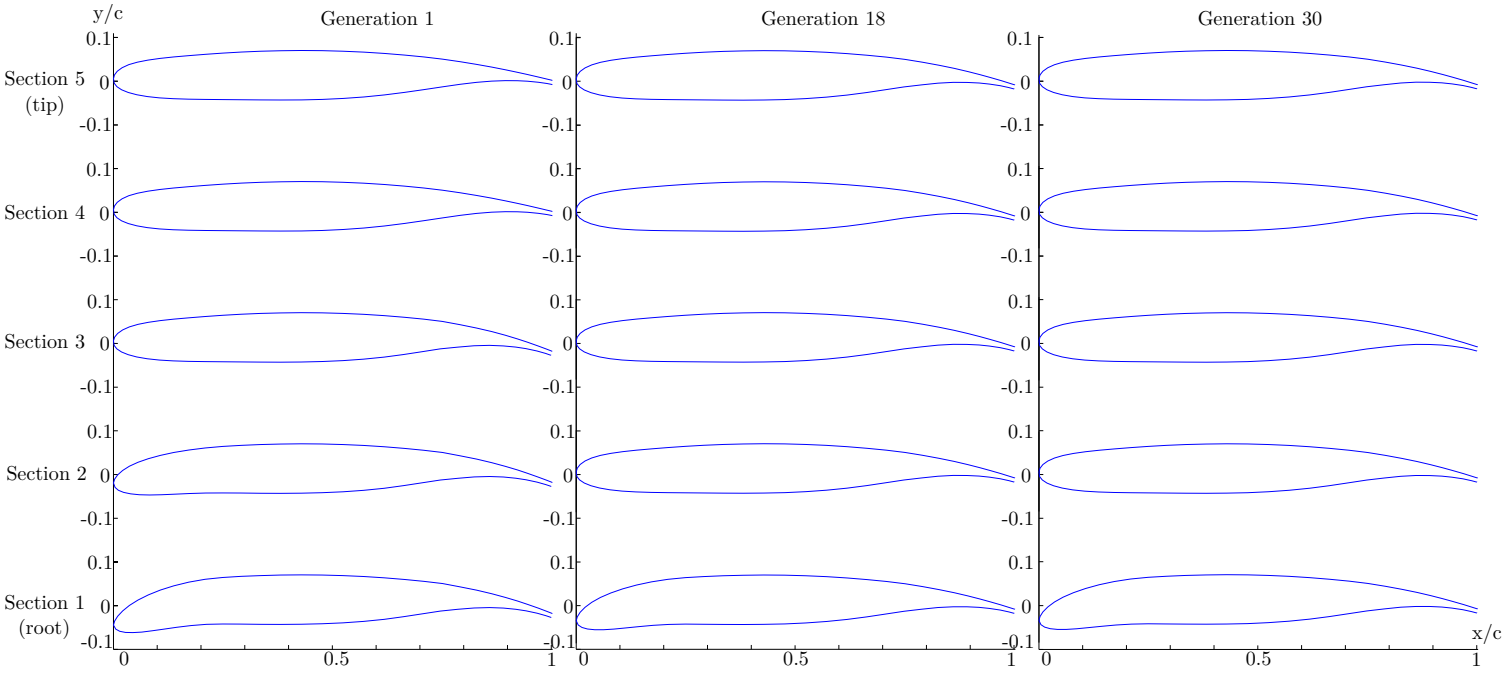

Fig. 19 Light cruise best individual evolution.

B. Wind tunnel experiment

Figures 20 and 21 show the lift and drag polars for the five tested configurations. Based on the drag equation $C_D = C_{D_0} + \frac{C_L^2}{\pi e AR}$, the drag polar equations were obtained by a second order polynomial fit of form $C_D = C_{D_0} + kC_L^2$. The fit coefficients are shown in Tab. 7.

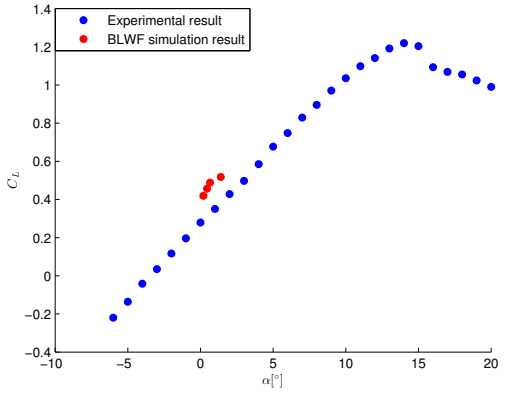

(a) Climb configuration

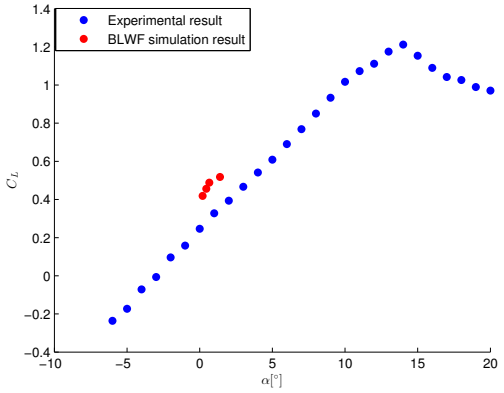

(b) Heavy cruise configuration

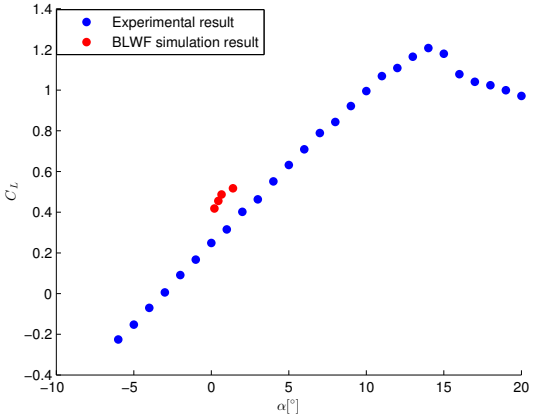

(c) Mid cruise configuration

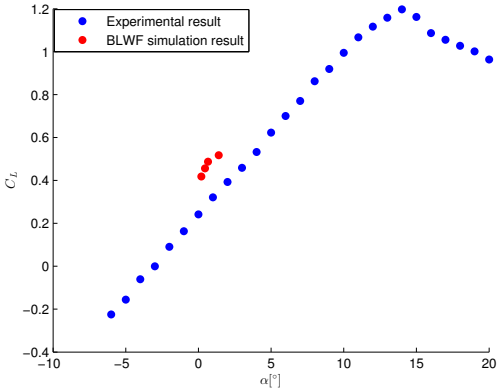

(d) Light cruise configuration

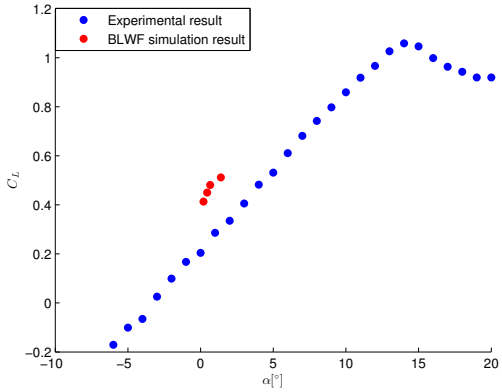

(e) Baseline configuration (No winglet)

Fig. 20 Lift as function of attack angle

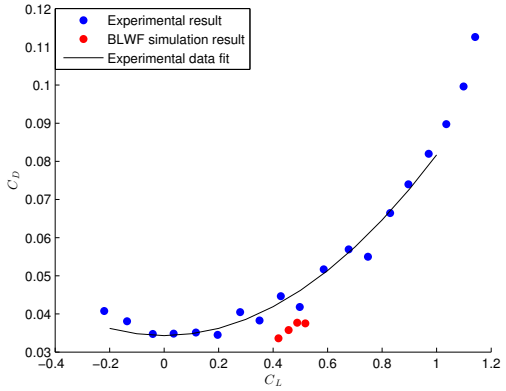

(a) Climb configuration

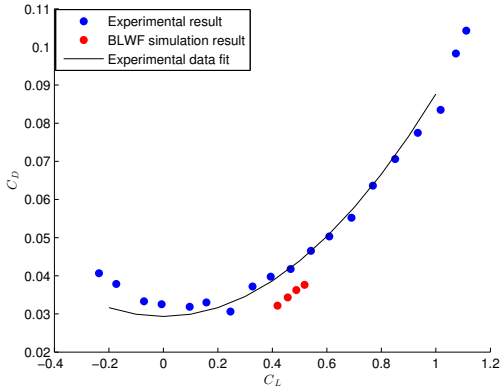

(b) Heavy cruise configuration

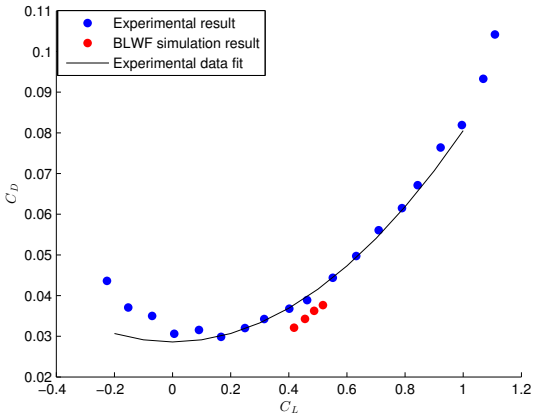

(c) Mid cruise configuration

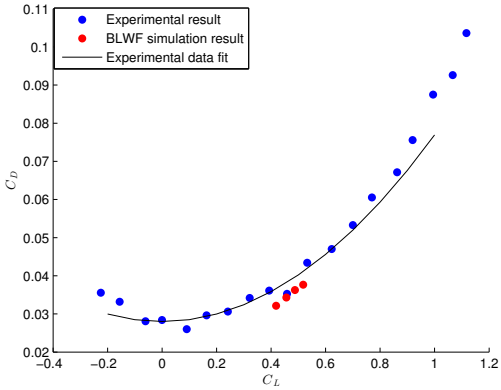

(d) Light cruise configuration

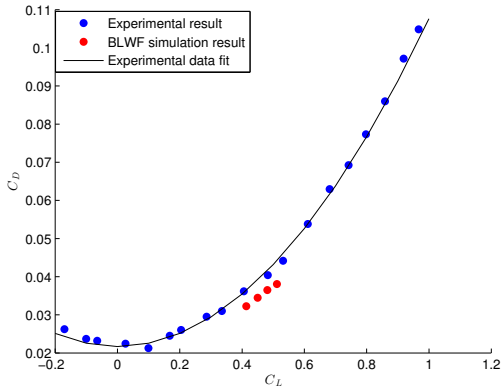

(e) Baseline configuration (No winglet)

Fig. 21 Drag polars

Table 7 Drag polar fit coefficients

Winglet geometry	C_{D_0}	k
No winglet	0.02169	0.08592
Climb	0.03432	0.04736
Heavy cruise	0.02932	0.05832
Mid cruise	0.02860	0.05194
Light cruise	0.02801	0.04890

An increase of C_{D_0} due the additional area is observed. A reduction of k show increased effective aspect ratio for all winglets. A reduction of C_{D_0} for smaller C_L conditions is achieved as a effect of the morphing feature of the winglets meaning that the winglet load is reduced while the airplane is flying at lower lift conditions without affecting the lift induced drag. This analysis shows that BLWF underestimates the lift and drag componets, resutls in agreement with Zhang and Hepperle [26].

Focusing on the C_L range of interest, Fig. 22, the light cruise winglet configuration shows smallest drag than all the other configurations. Other winglet configurations probably did not show the expected result due the differences of flow conditions between the wind tunnel test and actual flight conditions.

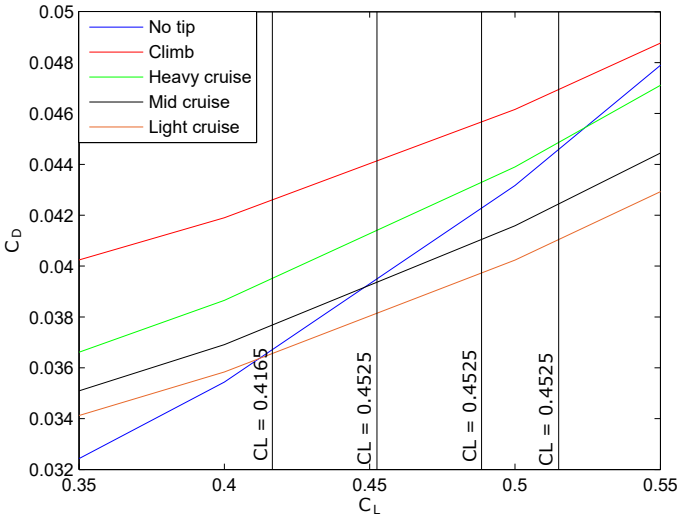

Fig. 22 Configurations drag comparison at the region of interest.

V. Conclusions

The genetic optimization results show that the use of a camber morphing winglet can improve the airplane aerodynamic performance, reducing the total drag up to 0.58% over an already optimized fixed geometry winglet. This result shows the capability of the camber morphing winglet to improve aircraft performance when compared to a mission optimized fixed geometry winglet. The results shows an encouraging scenario for testing the device on airplanes with higher wing loading, causing a bigger drag and fuel consumption reduction.

The wind tunnel results show that the expected increase on the C_{D_0}, due the surface area addition, and reduction of the lift induced drag compared to the wing with no tip device. The total drag is reduced in the optimization C_L region, despite the fact some of the winglets showing performance under the expected due the differences between the experiment and real flight conditions.

Further investigations on the performance of the morphing winglet for a complete flight and the estimation of the fuel consumption for a plane equipped with camber morphing winglets are expected as future steps of this research. Also, the procedure developed may be used for designing a new winglet for a new aircraft project.

VI. Acknowledgments

This work has been funded by the UTwente's International Strategic Partner Project Bandeirantes and the 4TU FSM center. The authors would like to thank S. Wanrooij and H. Stobbe for the technical support, L. H. Groot Koerkamp, M. M. Nilton, M. F. Cichocki and L. I. Abreu for support in the experiments setup.

References

[1] Kroo, I., "Nonplanar wing concepts for increased aircraft efficiency," VKI lecture series on innovative configurations and advanced concepts for future civil aircraft, June 2005.

[2] Chattot, J. J., "Low speed design and analysis of wing/winglet combinations including viscous effects," *Journal of Aircraft*, Vol. 43, No. 2, 2006, pp. 386–389. doi:10.2514/1.15349.

[3] Takenaka, K., Hatanaka, K., Yamazaki, W., and Nakahashi, K., "Multidisciplinary Design Exploration for a Winglet," *Journal of Aircraft*, Vol. 45, No. 5, 2008, pp. 1601–1611. doi:10.2514/1.33031.

[4] Céron-Muñoz, H. D., Cosin, R., Coimbra, R. F. F., Correa, L. G. N., and Catalano, F. M., "Experimental Investigation of Wing-Tip Devices on the Reduction of Induced Drag," *Journal of Aircraft*, Vol. 50, No. 2, 2013, pp. 441–449. doi:10.2514/1.C031862.

[5] Gagnon, H., and Zingg, D. W., "Two-Level Free-Form and Axial Deformation for Exploratory Aerodynamic Shape Optimization," *AIAA Journal*, Vol. 53, No. 7, 2015, pp. 2015–2026. doi:10.2514/1.J053575.

[6] Krebs, T., and Bramesfeld, G., "Using an optimisation process for sailplane winglet design," *The Aeronautical Journal*, Vol. 120, No. 1233, 2016, pp. 1726–1745. doi:10.1017/aer.2016.83.

[7] Reddy, S. R., Sobieczky, H., Dulikravic, G. S., and Abdoli, A., "Multi-Element Winglets: Multi-Objective Optimization of Aerodynamic Shapes." *Journal of Aircraft*, Vol. 53, No. 4, 2016, pp. 992–1000. doi:10.2514/1.C033334.

[8] Secanell, M., Suleman, A., and Gamboa, P., "Design of a Morphing Airfoil Using Aerodynamic Shape Optimization," *AIAA Journal*, Vol. 44, No. 7, 2006, pp. 1550–1562. doi:10.2514/1.18109.

[9] Gamboa, P., Vale, J., Lau, F. J. P., and Suleman, A., "Optimization of a Morphing Wing Based on Coupled Aerodynamic and Structural Constraints," *AIAA Journal*, Vol. 47, No. 9, 2009, pp. 2087–2104. doi:10.2514/1.39016.

[10] Beguin, B., C, B., and Adams, N., "Aerodynamic Investigations of a Morphing Membrane Wing," *AIAA Journal*, Vol. 50, No. 11, 2012, pp. 2588–2599. doi:10.2514/1.J051772.

[11] Previtali, F., Arrieta, A. F., and Ermanni, P., "Performance of a Three-Dimensional Morphing Wing and Comparison with a Conventional Wing," *AIAA Journal*, Vol. 52, No. 10, 2014, pp. 2101–2113. doi:10.2514/1.J052764.

[12] Molinari, G., Aarrieta, A. F., and Ermanni, P., "Aero-Structural Optimization of Three-Dimensional Adaptive Wings with Embedded Smart Actuators," *AIAA Journal*, Vol. 52, No. 9, 2014, pp. 1940–1951. doi:10.2514/1.J052715.

[13] Smith, D. D., Ajaj, R. M., Isikveren, A. T., and Friswell, M. I., "Multi-Objective Optimization for the Multiphase Design of Active Polymorphing Wings," *Journal of Aircraft*, Vol. 49, No. 4, 2012, pp. 1153–1160. doi:10.2514/1.C031499.

[14] Ursache, N., Melin, T., Isikveren, A. T., and Firswll, M. I., "Morphing Winglets for Aircraft Multi-Phase Improvement," *7th AIAA ATIO Conf, 2nd CEIAT Int'l Conf on Innov and Integr in Aero Sciences,17th LTA Systems Tech Conf; followed by 2nd TEOS Forum, Aviation Technology, Integration, and Operations (ATIO) Conferences*, 2007. doi:10.2514/6.2007-7813.

[15] Bourdin, P., Gatto, A., and Friswell, M. I., "Aircraft control via variable cant-angle winglets. Journal of Aircraft," *Journal of Aircraft*, Vol. 45, No. 2, 2008, pp. 414–423. doi:10.2514/1.27720.

[16] De Breuker, R., Abdalla, M., and Gurdal, Z., "Design of morphing winglets with the inclusion of nonlinear aeroelastic effects," *The Aeronautical Journal*, Vol. 115, 2011, pp. 713–728. doi:10.1017/S0001924000006461.

[17] Martins, A. L., and Catalano, F. M., "Drag optimization for transport aircraft Mission Adaptive Wing," *Journal of the Brazilian Society of Mechanical Sciences and Engineering*, Vol. 25, No. 1, 2003. doi:10.1590/S1678-58782003000100001.

[18] Cosin, R., Angelo, M. V., Catalano, F. M., and De Salvi, F. T. B., "Mission Adaptive Wing Optimization with Wind Tunnel Hardware in the Loop." *13th AIAA/ISSMO Multidisciplinary Analysis Optimization Conference*, 2010.

[19] Cayiroglua, I., and Kilic, R., "Wing Aerodynamic Optimization by Using Genetic Algoritm and Ansys," *3rd International Conference on Computational and Experimental Science and Engineering*, 2016.

[20] Holst, T. L., and Pulliam, T. H., "Transonic Wing Shape Optimization Using a Genetic Algorithm," *IUTAM Symposium Transsonicum IV*, Springer Netherlands, 2003, pp. 245–252.

[21] Karas, O. V., and Kovalev, V. E., *BLWF 58 User's Guide*, 2004.

[22] Johnson, F. T., Tinoco, E. N., and Yu, N. J., "Thirty years of development and application of CFD at Boeing commercial airplanes, Seattle," *Computers and Fluids*, 2005, p. 1115–1151.

[23] Jameson, A., and Caughey, D. A., "A Finite Volume Method for Transonic Potential Flow Calculations," *13th Fluid and PlasmaDynamics Conference*, 1977.

[24] McLean, J. D., and Randall, J. L., "Computer program to calculate three-dimensional boundary layer flows over wings with wall mass transfer." *NASA CR-3123*, 1978.

[25] Yu, N. J., "Grid generation and transonic flow calculations for three-dimensional configurations," 1980.

[26] Zhang, k.-s., and Hepperle, M., "Evaluation of the BLWF Code - A Tool for the Aerodynamic Analysis of Transonic Transport Aircraft COnfigurations," 2010.

[27] Roskam, J., and Lan, C., *Airplane Aerodynamics and Performance*, Design, Analysis and Research Corporation, 1997.

[28] Goldberg, D. E., *Genetic Algorithms in Search, Optimization, and Machine Learning*, Addison-Wesley Longman Publishing Co., Inc., 1989.

[29] Thierens, D., and Goldberg, D., "Convergence models of genetic algorithm selection schemes," *Parallel Problem Solving from Nature - PPSN III*, Springer Berlin Heidelberg, 1994, pp. 119–129.